Molecular theory of high elasticity of polymer nets with allowance for topological constraints

F. F. Ternovskiĭ and A. R. Khokhlov

Moscow State University

We propose a molecular theory of the nonlinear inelasticity of polymer nets having strongly tangled subchains, with allowance for the constraints imposed on the possible conformations by entanglement of various subchains (topological constraints). The analysis is based on the model of a polymer chain in a net of impenetrable obstacles, and permits calculation of the net's free elastic energy, which is found to depend on the method of network synthesis. We study the uniform swelling of the nets and the uniaxial tension and compression of a dry network produced by instantaneous crosslinking of polymer nets in a melt or solution, as well as of a swollen net. A molecular interpretation is offered of the known Mooney-Rivlin corrections in high-elasticity theory; it is shown that these corrections decrease for swollen nets as well as for dry nets prepared in the presence of a solvent. The theory proposed is compared with the experimental data.

1. INTRODUCTION

A polymer net (or gel) constitutes in the simplest case an aggregate of polymer chains crosslinked to one another by valent chemical bonds and forming a single three-dimensional body (see Fig. 1). The crosslinks can be produced, for example, by γ irradiation of a polymer solution or a melt; there are also many other methods.[1] The physical property of a polymer chain depend strongly on the method of its preparation.

If the crosslink density is low, the polymer chains have the property of high elasticity, i.e., the ability to withstand exceedingly high elastic strains in the region of the nonlinear dependence of the strains on the stresses. The development of a molecular theory of nonlinear high elasticity of polymer chains is one of the fundamental problems of macromolecule statistical physics.

The classical theory of high elasticity was developed in the 40s independently by a number of workers[2-5] (see also Ref. 6). The main simplification of the classical theory is the assumption that the subchains of a chain (i.e., chains between two neighboring crosslinks, can take on with equal probability an arbitrary conformation compatible with the given distance between the ends of the subchain, i.e., between the crosslinks that limit the subchain. The elasticity of a polymer chain is in this case of purely entropy nature and is produced because when the network is deformed the distances between crosslinks are correspondingly altered, thus decreasing the set of possible conformations for the aggregate of subchains. For uniaxial tension and compression of a dry (containing no solvent) polymer net, classical theory yields the following dependence of the stress τ (per unit cross-section area of the sample in the initial state) on the relative strain $\lambda = l/l_0$ (l_0 and l are the sample dimension in the direction of the stretching axis before and after application of the stress, respectively):

$$\tau = \nu T (\lambda - \lambda^{-2})/V_0, \tag{1}$$

where T is the temperature, ν the number of subchains in the sample, and V_0 its volume in the underformed state.

Relation (1) agrees well enough with the experimental data in the compression region ($\lambda < 1$), but at $\lambda > 1$ considerable deviations appear right away. These deviations are described by an empirical formula first proposed in Refs. 7 and 8 and known as the Mooney-Rivlin formula:

$$\tau = \nu T (\lambda - \lambda^{-2}) (c_1 + c_2 \lambda^{-1})/V_0, \tag{2}$$

where the constants c_1 and c_2 are in general of the same order of magnitude.

The explanation of this fact, as well as of a number of other observed deviations from the classical theory of high elasticity, is the subject of a large number of papers (see the review in Ref. 9). According to present-day notions, the reason for these deviations is that the individual subchains of the polymer chain are strongly intertwined; since one chain cannot pass unbroken through another, not all possible conformations of a given subchain can be realized, and con-
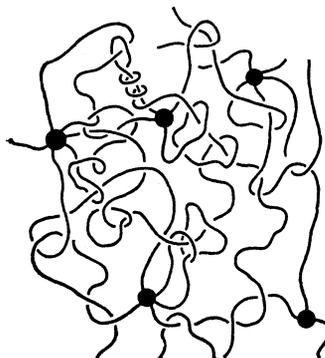

FIG. 1. Schematic representation of polymer gel.
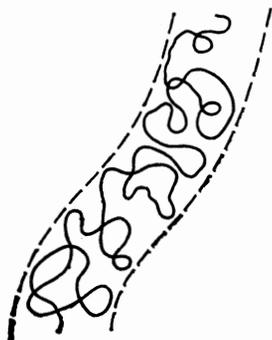
0038-5646/86/040728-09$04.00

FIG. 2. Model of "polymer chain in a tube."

straints, called topological, are imposed on choice of the conformations.

In the papers of the last few years topological constraints are described as a rule within the framework of the model of a "polymer chain in a tube" (see Fig. 2). It is assumed that for each subchain there exists some preferred contour that joins its ends (the axial line of the tube in Fig. 2: this contour is also called the primitive path). The topological constraints permit only relatively small fluctuations of the subchain about this contour; it is this circumstance that is simulated by regarding each subchain as enclosed inside a certain tube of finite diameter (see Fig. 2). In theories based on this model (see Refs. 10–15) the possible set of conformations of each subchain turns out to be substantially smaller than in the classical theory.

In a number of cases, theories that use the model of a "polymer chain in a tube" make it possible to improve somewhat the agreement with experiment when individual properties of high-elasticity polymer nets are described. A careful analysis of the entire assembly of these properties,[16,17] however, has shown that none of the theories in Refs. 10–15 can claim satisfactory agreement with experiment. This is not surprising, since the tube model is a rather crude approximation of the real situation and should furthermore, when nonlinear properties are studied, be supplemented by a number of phenomenological assumptions that are unfounded from the molecular viewpoint (see Ref. 18).

The present paper is devoted to the development of a molecular theory of high elasticity of polymer nets on the basis of a new microscopic model that describes the real situation much more fully than the tube model. Assume that each subchain of the net constitutes a random walk through a framework of straight lines that are the edges of a cubic lattice (see Fig. 3a; Fig. 3b shows a two-dimensional variant of this model). The topological constraints are simulated here by the fact that as the polymer chain moves it cannot cross any obstacle (a straight line in Fig. 3a or a point in Fig. 3b). As a result, the set of conformations of a subchain with fixed end points becomes much smaller. Clearly, our model has a number of important advantages over the "chain in a tube" model: a) the unphysical concept of tube thickness does not enter explicitly in our model; b) the tube walls in this model are not continuous—parts of the chain can "leak out" through the gaps between the fixed crosslinks, form

sections of spare length (or loops); c) in our model we can consider in a natural manner the cases of relatively short subchains, with only a few crosslinks per chain, etc. We shall show next that the model shown in Fig. 3 can be used, without additional phenomenological parameters, to construct for highly elastic properties of polymer nets a theory that describes a large group of experimental data. Moreover, it becomes possible, for the first time ever, to investigate on the molecular level within the framework of this theory the dependence of the elastic properties of nets on a number of characteristics of the process of their preparation. The formulation of the problems of the theory of high elasticity for the model shown in Fig. 3 poses also a number of interesting problems of general physical character.

It should be noted that the behavior of a polymer chain inside a lattice of uncrossable obstacles was investigated in a number of recent papers,[19-22] but this model was not considered before as applied to high-elasticity theory.

2. FREE ENERGY OF A POLYMER NET

We proceed now to a quantitative formulation of the problem. We assume that in the initial (undeformed) state each subchain of the polymer net is in a lattice of obstacles, as shown in Fig. 3. We assume for simplicity that all the subchains of the net are equal and contain N links, each with dimension a. We denote also by c the period of the obstacle lattice. We suppose that the net is weakly crosslinked, so that the subchains are long enough, $Na^2 \gg c^2$, i.e., each subchain occupies many cells of the obstacle lattice. In a concentrated polymer system such as a polymer net, it is permissible to disregard in first-approximation analysis of the high elasticity the volume interactions of the links.[1] Individual chains
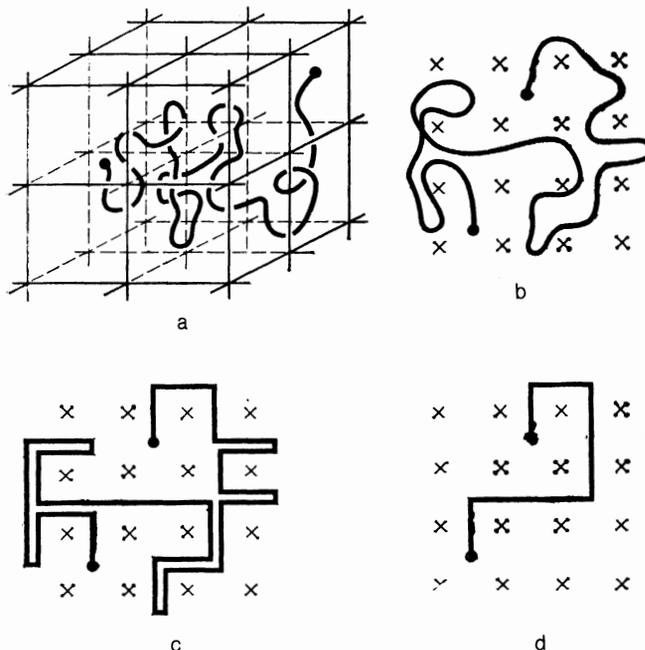

FIG. 3. Polymer chain in a lattice of obstacles: a—three-dimensional case; b—two-dimensional case; c—coarsened trajectory of chain; d—primitive path of chain.

F. F. Ternovskiĭ and A. R. Khokhlov   729

will therefore be regarded as statistically independent.

We introduce a coordinate frame connected with the obstacle lattice, and assume that we have applied to the net a certain stress that changed the dimensions of the sample, along each of the coordinate axes, by a factor λ_i ($i = x, y, z$ in the three-dimensional case). The simplest examples are here: isotropic swelling ($\lambda_x = \lambda_y = \lambda_z$) and uniaxial tension or compression of a dry net. The latter takes place at a constant sample volume (since dry net respond very weakly to isotropic compression), so that in the three dimensional case we have $\lambda_x = \lambda$, $\lambda_y = \lambda_z = \lambda^{-1/2}$. It is natural to expect the obstacle lattice to be deformed affinely with the net sample. Thus, in the deformed state its unit cell is a right parallelepiped with sides $\lambda_i c$.

In the presence of a lattice of topological constraints, the partition function of a subchain of N steps with fixed end points, which coincides in our case with the number of possible conformations, depends not only on the arrangement of the end points of the subchains (just as in classical theories), but also on form of the trajectory of the chain between these points. To cast light on this circumstance, consider Fig. 3. Figure 3b shows the true microscopic trajectory of a subchain (for simplicity, in a two-dimensional case), while Fig. 3c shows the same trajectory, but "coarsened" to a scale c (i.e., with trajectory details of scale smaller than c left out). Further coarsening can be achieved by eliminating from Fig. 3c all the loop sections of the trajectory, i.e., those sections on which the trajectory is closed and not crosslinked with any of the obstacles (see Fig. 3d). The trajectory obtained on Fig. 3c will hereafter be called coarsened, and that of Fig. 3d the primitive path of the given subchain (cf. Refs. 19–21). Note that all the subchain conformations having one and the same primitive path are topologically equivalent, i.e., they can be obtained one from another by continuously deforming the trajectory without crossing the obstacle lattice. It is readily understandable that it is just the primitive path of each subchain which is invariant to deformation of a polymer chain, and that the partition function of the subchain is a functional of its primitive path.

We shall show later that out of all the characteristics of the primitive path, the partition function of the subchain numbered α ($\alpha = 1, 2, ..., \nu$, cf. (1) and (2)) depends only on the numbers $k_{\alpha i}$ of steps that the primitive path makes along the coordinate axes ($k_x = 3$ and $k_y = 4$ in Fig. 3d). Thus, $Z_\alpha = Z(N, \mathbf{k}_\alpha)$, $\mathbf{k}_\alpha$ is a vector with coordinates $k_{\alpha i}$, and the partition function of the net is, by virtue of the statistical independence of the subchains,

$$Z = \prod_{\alpha=1}^{\nu} Z(N, \mathbf{k}_\alpha). \tag{3}$$

We denote by $\nu(\mathbf{k})$ the number of chains in a net with primitive paths characterized by parameters k_i, and by $P(\mathbf{k}) = \nu(\mathbf{k})/\nu$ the corresponding distribution of the primitive paths in k_i. This distribution is determined by the method used to prepare the net; it is not altered by elastic deformation of the latter. We can then write for the free energy $\mathcal{F} = -T \ln Z$ of the polymer net, taking (3) into account,

$$\mathcal{F} = -\nu T \sum_{k_i} P(\mathbf{k}) \ln Z(N, \mathbf{k}). \tag{4}$$

We proceed to calculate the partition function $Z(N, \mathbf{k})$. We denote by Q_i the total number of steps of the coarsened trajectory (see Fig. 3c) taken along the ith coordinate axis. Some of these steps belong to the primitive path, and the remainder pertain to the loop sections. Therefore the difference $Q_i - k_i$ is a non-negative even number. Even for a fixed topological state (primitive path) of the considered subchain, the quantities Q_i do not remain unchanged on deformation, meaning that the loop sections become redistributed.

In the deformed states, the steps of the coarsened trajectory along the different coordinate axes are generally speaking not on a par, since their lengths λ_{ic} are different. Therefore different numbers of polymer-chain links go to these steps on the average; we denote the corresponding quantities by G_i. Since the total number of subchain links is N, we should have in any conformation

$$\sum_i Q_i G_i = N. \tag{5}$$

Next, along each of the axes, a coarsened-trajectory step containing G_i steps of the true (microscopic) trajectory can be effected by many different methods. To take this circumstance into account we assign to each coarsened-trajectory step along the ith coordinate axis a weight p_i. Then the total coarsened trajectory corresponds to a weight $\prod_i p_i^{Q_i}$. The calculation of p_i is considered in Sec. 4.

Taking the foregoing into account, we can write the partition function of a subchain in an obstacle lattice in the form

$$Z(N, \mathbf{k}) = \Gamma \sum' \prod_i p_i^{q_i} Y(\mathbf{Q}, \mathbf{k}), \tag{6}$$

where Γ is the total number of conformations of a chain of N links, $Y(\mathbf{Q}, \mathbf{k})$ is the number of methods of realizing the coarsened trajectory with Q_i steps along the axes for a specified primitive path (with parameters k_i. The prime on the summation sign means that the summation is over all possible values of Q_i that satisfy condition (5).

This condition can be taken into account by writing

$$Z(N, \mathbf{k}) = \frac{\Gamma}{2\pi i} \oint \frac{dx \, w(\mathbf{q}, \mathbf{k})}{x^{N+1}}, \tag{7}$$

where $\mathbf{q}$ is a vector with components

$$q_i = p_i x^{G_i}, \tag{8}$$

and $w(\mathbf{q}, \mathbf{k})$ is the generating function for the quantities $Y(\mathbf{Q}, \mathbf{k})$:

$$w(\mathbf{q}, \mathbf{k}) = \sum_{Q_i=0}^{\infty} \prod_i q_i^{q_i} Y(\mathbf{Q}, \mathbf{k}). \tag{9}$$

The integration in (7) is along a closed loop enclosing the point $x = 0$ and located in its entirety inside the convergence region of the series (9).

Allowance for the supplementary condition (5) reduces thus to the renormalization (8) of the statistical weights p_i. The sum (9) will be calculated in the next section, where we shall use a generalization of a method proposed in Ref. 9.
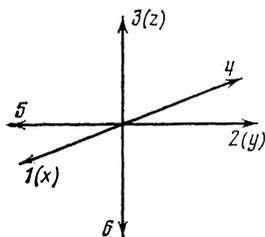
FIG. 4. Method of numbering the direction for a three-dimensional cubic lattice of obstacles ($\sigma = 3$).

3. POLYMER CHAIN IN A LATTICE OF OBSTACLES

We denote by 2σ the number of directions in which each next step of the coarsened trajectory in Fig. 3c can be made. We assign a separate number for each direction, and assign numbers that differ by σ to opposing directions. In the usually case, for a cubic lattice of obstacles we have $\sigma = 3$ and the method of numbering the direction is indicated in Fig. 4. We shall indicate in the present section the method of calculating sums over coarsened trajectories of definite classes, with each trajectory entering with a weight

$$\prod_{i=1}^{2\sigma} q_\nu^{L_\nu},$$

where q_ν is the weight of a step in the direction ν, and L_ν is the number of steps in this direction. The general results are of interest to us primarily as applied to the calculation of the sum (9), in which case $q_\nu = q_{\nu+0}$. For example, for a three-dimensional cubic lattice of obstacles,

$$q_1 = q_4 = q_x, \quad q_2 = q_5 = q_y, \quad q_3 = q_6 = q_z,$$
$$L_1 + L_4 = Q_x, \quad L_2 + L_5 = Q_y, \quad L_3 + L_6 = Q_z. \quad (10)$$

We introduce the following definitions:

1. $A_\nu(2m)$—sum (in the sense indicated above) over all the closed trajectories (loops) not crosslinked with obstacles, having a length $2m$ and satisfying two conditions: a) the first step is made in the ν direction, b) the trajectory lands for the first time on the initial point after the last step. By definition, $A_\nu(0) = 0$.

2. $B_\nu(2m)$—sum over all closed trajectories, not crosslinked with obstacles, having a length $2m$ and returning to the initial point (not necessarily for the first time) from all directions except a forbidden one whose number is ν. By definition, $B_\nu(0) = 1$.

3. $C(2m)$—sum over all possible not crosslinked closed trajectories of length $2m$; $C(0) = 1$.

It is easily established that the quantities A_ν, B_ν, and C satisfy the following recurrence relations:

$$A_\nu(2m) = q_\nu q_{\nu+\sigma} B_\nu(2m-2),$$

$$B_\nu(2m) = \sum_{\mu \neq \nu} \sum_{n=0}^{m} A_\mu(2m-2n) B_\nu(2n),$$

$$C(2m) = \sum_{\mu} \sum_{n=0}^{m} A_\mu(2m-2n) C(2n),$$

(cf. Ref. 19). These recurrence relations can be solved by using the method of generating functions we put

$$A_\nu, B_\nu, C(y) = \sum_{m=0}^{\infty} A_\nu, B_\nu, C(2m) y^{2m}. \quad (11)$$

Using the recurrence relations, we obtain

$$A_\nu(y) = y^2 q_\nu q_{\nu+\sigma} B_\nu(y), \quad (12)$$

$$B_\nu(y) = 1 + [A(y) - y^2 q_\nu q_{\nu+\sigma} B_\nu(y)] B_\nu(y), \quad (13)$$

$$C(y) = 1 + A(y) C(y), \quad (14)$$

where we have put

$$A(y) = \sum_{\nu} A_\nu(y). \quad (15)$$

Solving the system (12)—(15), we can easily obtain all the functions of interest to us. To save space we shall not write out the corresponding solution in explicit form. We note only that we always have

$$A_\nu(y) = A_{\nu+\sigma}(y), \quad B_\nu(y) = B_{\nu+\sigma}(y). \quad (16)$$

In the case $q_1 = ... = q_{2\sigma} = 1$ we get $A_1 = ... = A_{2\sigma} = A/2\sigma$, $B_1 = ... B_{2\sigma} = B$, where the functions A, B, and C coincide with the corresponding functions obtained in Ref. 19.

We turn now to the calculation of the sum (9). This is in fact a weighted sum over all possible trajectories obtained by adding all possible non-crosslinked loops to the primitive path, which we assume here to be specified by a sequence of directions ν_1, ν_2, ..., ν_k. Using the quantities $C(2m)$ and $B_\nu(2m)$ introduced above, we can represent the sum of interest to us in the form

$$w(\{q_\nu\}, \nu_1, \nu_2, \ldots, \nu_k)$$
$$= q_{\nu_1} q_{\nu_2} \ldots q_{\nu_k} \sum_{m_0, m_1, \ldots, m_k = 0}^{\infty} C(2m_0) B_{\nu_1}(2m_1) \ldots B_{\nu_k}(2m_k). \quad (17)$$

This equation is illustrated in Fig. 5. Taking the definitions (11) into account, we can represent the right-hand side of (17) in the form

$$C(y=1) \prod_{\nu} [q_\nu B_\nu(y=1)]^{l_\nu},$$

where l_ν is the number of primitive-path steps in the ν direction. We have thus proved that the only primitive-path characteristic on which the sum w (and hence the partition) depends are the numbers l. In the case $q_\nu = q_{\nu+\sigma}$, taking (16)
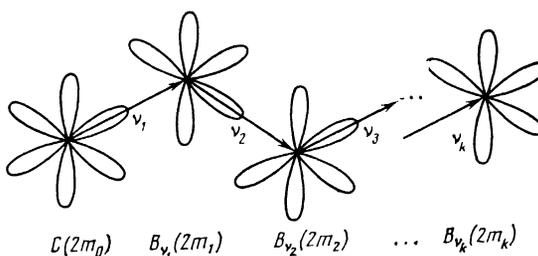

$$C(2m_0) \quad B_{\nu_1}(2m_1) \quad B_{\nu_2}(2m_2) \quad \ldots \quad B_{\nu_k}(2m_k)$$

FIG. 5. Illustration for Eq. (17).

into account, we see that w depends only on the numbers $k_v = l_v + l_{v+\sigma}$. This is precisely the situation when the partition function (7) is calculated. As a result we obtain

$$Z(N,\mathbf{k}) = \frac{\Gamma}{2\pi i} \oint \frac{dx\, C(y=1)}{x^{N+1}} \prod_{i=1}^{\sigma} [q_i B_i(y=1)]^{k_i}. \quad (18)$$

The quantities $C(y=1)$ and $B_i(y=1)$ can be easily determined from the system (12)–(15). Putting $A(y=1) = 1 - 2u$ we obtain

$$C(y=1) = 1/2u, \qquad B_i(y=1) = 1/[u+(u^2+q_i^2)^{1/2}], \quad (19)$$

where u is the non-negative solution of the equation

$$(\sigma-1)u+1/2 = \sum_{i=1}^{\sigma} (u^2+q_i^2)^{1/2}. \quad (20)$$

We recognize now that in the case $Na^2 \gg c^2$ considered the characteristic values $k_i \gg 1$. Therefore the integral (18) can be calculated by the saddle-point method. The result is of the form

$$\ln Z(N,\mathbf{k}) = -N\ln x + \sum_i k_i \ln\{q_i[u+(u^2+q_i^2)^{1/2}]^{-1}\} + \ln\Gamma, \quad (21)$$

where the value of x is determined from the condition that $\ln Z(N,\mathbf{k})$ be a maximum with respect to x:

$$\partial \ln Z(N,\mathbf{k})/\partial x = 0. \quad (22)$$

We have left out of (21) terms of order $\ln N$, which do not contribute to the thermodynamic quantities.

Equation (22) can be represented in the form

$$\sum_i G_i \bar{Q}_i = N, \quad (23)$$

where the quantities

$$\bar{Q}_i = q_i \partial \ln Z(N,\mathbf{k})/\partial q_i \quad (24)$$

have the meaning of the mean values of the numbers of steps of the coarsened trajectory along the i axis in conformations with the given primitive path.

Let us dwell also on the method of determining the numbers G_i of links per step of the coarsened trajectory (along the i axis). Within the framework of our approach it is natural to regard these parameters as variational and choose them to satisfy the condition that the number of conformations $Z(N,\mathbf{k})$ for the given primitive path be a maximum: $\partial \ln Z(N,\mathbf{k})/\partial G_i = 0$. Taking (8), (21), and (22) we obtain

$$\partial \ln p_i/\partial G_i + \ln x = 0. \quad (25)$$

4. STATISTICAL WEIGHT OF A COARSENED-TRAJECTORY STEP

To calculate the partition function $Z(N,\mathbf{k})$ in explicit form it remains to find the statistical weights p_i for the steps of the coarsened trajectory. In accordance with the meaning of expression (6), the quantity $\Gamma \prod_i p_i^{Q_i}$ should be identified with the number of microconformations of a chain having a

coarsened trajectory with parameters Q_i. An approximate method of calculating p_i is described in this section.

Generally speaking, any subchain conformation corresponding to a given roughened trajectory can be subdivided into individual segments $\mathbf{r}_0 - \mathbf{r}_1$, $\mathbf{r}_1 - \mathbf{r}_2, ..., \mathbf{r}_{Q-1} - \mathbf{r}_Q$ ($\Sigma_i Q_i = Q$) such that the vector $\mathbf{r}_{s-1} - \mathbf{r}_s$ joins the same cells of the obstacle lattice as the sth step of the coarsened trajectory. The sum over all the microconformations of a subchain for a given coarsened trajectory is thus the sum over all possible conformations of the segments of the chains between the points $\mathbf{r}_{s-1}$ and $\mathbf{r}_s$ and over all possible positions of the points $\mathbf{r}_s$ ($s = 1, 2, ..., Q$) in the corresponding cells of the obstacle lattice. For an approximate analytic calculation of this sum we make the following assumptions (an exact calculation is possible only by numerical means, but the proposed simple analytic method discerns the main qualitative features): a) we assume that the chain segment between the points $\mathbf{r}_{s-1}$ and $\mathbf{r}$ contains exactly G_{i_s} links (i_s is the number of the axis along which the sth steps of the coarsened trajectory is directed); b) we assume that all the conformations of the chain segment of G_{i_s} links between the points $\mathbf{r}_{s-1}$ and $\mathbf{r}_s$ correspond to the given coarsened trajectory. Under these assumptions, the number R of microconformations, which corresponds to the given coarsened trajectory, is

$$R = \frac{\Gamma}{v_0} \int_{v_0} d^2\mathbf{r}_0 \int_{v_1} d^3\mathbf{r}_1 ... \int_{v_Q} d^3\mathbf{r}_Q \prod_{s=1}^{Q} \left(\frac{3}{2\pi a^2 G_{i_s}}\right)^{3/2}$$
$$\times \exp\left[-\frac{3(\mathbf{r}_{s-1}-\mathbf{r}_s)^2}{2a^2 G_{i_s}}\right], \quad (26)$$

where $v_0, v_1, ..., v_Q$ are the volumes of the obstacle-lattice cells through which the roughend trajectory of Q steps passes in succession. On the other hand, according to our definition of the weights p_i we should have

$$R = \Gamma \prod_i p_i^{Q_i}. \quad (27)$$

The Gaussian functions cannot be analytically integrated over the bounded volumes $v_0, v_1, ..., v_Q$ in (26). To simplify the resultant equations we assume that these integrations should be carried out over all of space, but with a suitable Gaussian weight:

$$\int_{v_s} d^3\mathbf{r}_s = \int d^3\mathbf{r}_s (2\pi)^{-3/2} \exp\left\{-\sum_i [(\mathbf{r}_s)_i - (\mathbf{r}_{0s})_i]^2 (2\delta_i^2)^{-1}\right\}, \quad (28)$$

where $(\mathbf{r}_{0s})_i$ are the Cartesian coordinates of the center of that obstacle-lattice cell in which the coarsened trajectory landed after s steps, and δ_i is the characteristic dimension of the obstacle-lattice cell along the i axis. Since we assume that the obstacle-lattice cell is affinely deformed together with the net sample, we put

$$\delta_i = b\lambda_i, \quad (29)$$

where b is the characteristic dimension of the integration volumes in (26) in the undeformed state. It is most natural to assume that this dimension coincides with the dimension

of the cells themselves, so that $b \sim c$. We shall not specify here more accurately the values of the parameters b/c (they are of the order of unity); this parameter will be used for adjustment when comparing the theoretical and experimental results (see Sec. 6).

If the approximation (28) is used, the integral (26) becomes Gaussian with infinite limits and can be exhaustively investigated. The result of such an investigation is that for a primitive path of arbitrary form the value of R cannot be represented in the form (27); this demonstrates the approximate character of expression (6) for the partition function of the subchain. To determine the statistical weights p_i in an approximation conforming to the approximation (6), it is reasonable to use the following method. We calculate R for a straight-line coarsened trajectory along an appropriate axis ($Q_i = Q, Q_j = 0$ at $j \neq i$) and equate it to the expected value

$$R = \Gamma p_i{}^Q. \qquad (30)$$

In this case R can indeed be represented in the form (30), with

$$p_i = B \prod_j D\left(\frac{g_i}{\alpha \lambda_j{}^2}\right) \exp\left(\frac{-3\lambda_i{}^2}{2g_i}\right), \qquad (31)$$

where we have introduced the notation

$$\alpha = 12b^2/c^2, \quad g_i = a^2 G_i/c^2, \quad D(t) = [t^{1/2} + (t+1)^{1/2}]^{-1}, \qquad (32)$$

and B is a normalization constant that can be determined by starting from the condition $p_i = 1/2\sigma$ in the undeformed state.

A detailed analysis shows that the assumption of a straight-line coarsened trajectory is optimal for the calculation of the statistical weights p_i from the point of view of all the assumptions made; attempts to take into account in one form or another the turns of the coarsened trajectory cannot be made in a noncontradictory manner, and are a patent exaggeration of the accuracy of the entire theory.

5. AVERAGING OVER THE PRIMITIVE PATHS

To calculate the free energy (4) of a polymer net we must average the logarithm (21) of the partition function over the primitive path distribution $P(k)$. This distribution, generally speaking, depends on the method of preparing the net. In contrast to the earlier treatments,[9-15] our approach takes into account the dependence of the net properties on the conditions of its preparation not via phenomenological parameters but directly with a molecular approach.

Consider, first, polymer nets obtained by instantaneous crosslinking in a dry undeformed state. That distribution of the primitive paths in k_i, which obtains under conditions of random walks of the polymer chain in the undeformed obstacle lattice, is then "frozen." This distribution was investigated in Refs. 19–21. It can be shown that for a three-dimensional cubic lattice of obstacles this distribution has at $Na^2 \gg c^2$ a sharp maximum of width[1] $\sim k^{1/2}$ near the point

$$k_i = k_0/3 = 2N/9G_0, \qquad (33)$$

where G_0 is the number, determined from (25), of links per step of the coarsened trajectory in the initial undeformed

state. The averaging in Eq. (4) can therefore be carried out for this case by directly substituting the values (33) in the expression for $\ln Z$:

$$\mathscr{F} = -\nu T \ln Z(N, \mathbf{k})|_{k_i = k_0/3}. \qquad (34)$$

As another example we consider networks obtained by instantaneous crosslinking in a concentrated polymer solution. Naturally, in this case the polymer chains are much less entangled than in crosslinking in the dry state, and the characteristic values of k_i for them are much smaller than in (34). However, since the crosslinking is instantaneous, the obtained distribution $P(k)$ is as before a frozen distribution for random walks of the polymer chain in the initial undeformed obstacle lattice, but now the period c of this lattice and the quantity $G_0 \propto c^2$ (to avoid confusion, we shall hereafter designate these quantities by $\bar{c}$ and $\bar{G}_0$) turn out to be larger than for crosslinking in the dry state. The maximum of the $P(k)$ distribution is then at the point

$$k_i = 2N/9\bar{G}_0 = \varepsilon k_0/3, \qquad (35)$$

where the parameter $\varepsilon = c^2/\bar{c}^2$ characterizes the degree of concentration of the polymer solutions under the crosslinking conditions.[2] We have therefore for the free energy

$$\mathscr{F} = -\nu T \ln Z(N, \mathbf{k})|_{k_i = \varepsilon k_0/3}. \qquad (36)$$

For an arbitrary method of net preparation one should naturally expect the distribution of the primitive paths in k_i not to coincide, generally speaking, with that obtained for free random walk in an arbitrary obstacle lattice. It can be assumed, however, that in many cases this distribution is isotropic and has a sharp maximum. For the free energy of a polymer net we can use, as before, Eqs. (35) and (36) and regard the parameter ε as a phenomenological one that characterizes the degree of entanglement of the chains of the net at the given method of its preparation.

Equations (33), (34) and (35), (36), (20)–(25) and (31) determine completely the free energy of a polymer net with arbitrary deformation characterized by the parameters λ_i. Calculations with these formulas were found to be feasible and were performed with a minicomputer. The results are presented in the next section (the obstacle-lattice cell was assumed three-dimensional cubic in all cases).

6. DISCUSSION OF RESULTS AND COMPARISON WITH EXPERIMENT

1. The simplest application of the expounded theory is consideration of isotropic swelling of a net obtained with instantaneous crosslinking in the dry state. In this case $\varepsilon = 1$, $\lambda_x = \lambda_y = \lambda_z = m$, $G_x = G_y = G_z = G = c^2 g/a^2$, $\bar{Q}_x = \bar{Q}_y = \bar{Q}_z/\bar{Q}/3, \bar{Q} = N/G$. The results for this case are shown in Fig. 6. Figure 6a shows the $g(m^2)$ dependence ($m > 1$ in the case of swelling, but we can carry out formally the calculations also for $m < 1$). At $m \ll 1$ we get, as we should, $g \propto m^2$. At $m > 1$, in view of the increased length of the primitive-path sections, the loop sections gradually vanish, the total number of steps of the coarsened trajectory becomes equal to $\bar{Q} = k_0$, and G reaches saturation $G = N/k_0 = 3G_0/2$. Figure 6b shows the dependence on m^2 of the
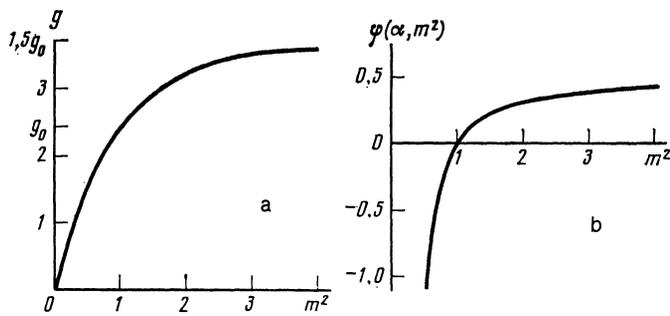
FIG. 6. Isotropic swelling of polymer net: plots of $g(m^2)$ (a) and of $\varphi(\alpha, m^2)$, (b) calculated at $\alpha = 12$ and $\varepsilon = 1$.

directly measurable quantity (see, e.g., Ref. 23) quantity

$$S = (1/mV_0)\partial\mathcal{F}/\partial m = (\nu NT/V_0 G_0)\varphi(\alpha, m^2),$$

$$\varphi(\alpha, m^2) = (3g_0/m^2 g)\{m^2/g - [g/(g+\alpha m^2)]^{1/2}\}.$$

As it should be when $Na^2 \gg c^2$, in the case of instantaneous crosslinking in the dry state, which freezes the free distribution of the chains, we have $\varphi(\alpha, 1) = 0$. As $m \to 0$ we have $\varphi(\alpha, m^2) \propto m^{-4}$, and at $m \gg 1$ we get $\varphi(\alpha, m^2) = 4/3g_0$.

If the crosslinking conditions are such that $\varepsilon \neq 1$ [see Eqs. (35) and (36)], we get

$$S = (\nu NT/V_0 G_0)\varepsilon^2\varphi(\alpha, \varepsilon m^2).$$

Thus, at $\varepsilon < 1$ not too strong a swelling decreases the elastic part of the free energy $(S < 0)$, whereas at $\varepsilon > 1$ the elastic part of the free energy always increases on swelling $(S > 0)$.

2. We consider now uniaxial tension and compression of a dry net obtained by instantaneous crosslinking in the dry state. In this case $\varepsilon = 1$, $\lambda_x = \lambda$, $\lambda_y = \lambda_z = \lambda^{-1/2}$. The dashed lines in Fig. 7 show the obtained dependence of the parameters $g_1 = a^2 G_x/c^2$, $g_2 = a^2 G_y/c^2 = a^2 G_z/c^2$ on λ^{-1}. It can be seen that at λ^{-1} values not greatly differing from unity the numbers of subchain links per step of the coarsened trajectory in various directions are far from equal. As $\lambda \to 0$ we have $g_1 \propto \lambda^2$, $g_2 = 9g_0/4$. As $\lambda \to \infty$ we have $g_1 = 9g_0/2$, $g_2 \propto \lambda^{-1}$. It can be seen from the figure that these theoretical limiting relations are not realized in fact at the experimentally attainable deformations. At $\lambda = 1$ we have $\bar{Q}_x = \bar{Q}_y = \bar{Q}_z = N/3G_0 = k_0/2$. The behavior of the quantity $l_i = Q_i(\lambda)/Q_i(1)$ is shown in Fig. 7a (dotted). When the loops having sections parallel to the i axis vanish, we should have $\bar{Q}_i = k_i = k_0/3$ and $l_i = 2/3$. Thus, under strong tension $(\lambda^{-1} \to 0)$ all the loops that are not crosslinked $(l_1 = l_2 = 2/3)$ become disentangled, while under strong compression $(\lambda^{-1} \to \infty)$ the loop sections perpendicular to the deformation axis vanish $(l_2 = 2/3)$, but many loops $(l_1 \to \infty)$ parallel to the deformation axis are formed.

The nonmonotonic variation of $l_2(\lambda^{-1})$ in the tension region is due to the fact that at first $\bar{Q}_2(\lambda^{-1})$ increases because the steps along the axes y and z become shorter, but subsequently all the loops parallel to the x axis become disentangled (l_1 decreases to the value 2/3) and with further tension the material to fill the long sections of the primitive path is drawn from disentanglement of the remaining loops.

In the physics of highly elastic polymer net the dependence of the elastic stress $\tau = (1/V_0)\partial\mathcal{F}/\partial\lambda$ on the relative strain is customarily described in terms of the so-called Mooney-Rivlin coordinates (ξ, λ^{-1}). Here $\varepsilon = \tau/\tau_0$, where τ_0 is the corresponding expression of the classical theory [see (1)]. The deviations of the $\xi(\lambda^{-1})$ plot from a straight line parallel to the abscissa axis describe the corrections to the classical behavior. According to the phenomenological Mooney-Rivlin formula (2), which describes well the experimental data in the tension region $(\lambda^{-1} < 1)$, the plot of $\xi(\lambda^{-1})$ in this region should be a straight line with a slope determined by the coefficient c; in the $\lambda^{-1} > 1$ region, however, the classical theory works well, so that the $\xi(\lambda^{-1})$ dependence is quite weak. These data agree well with the $\xi(\lambda^{-1})$ dependence calculated by us (for the case $\alpha = 12$, $\varepsilon = 1$), shown by the solid line in Fig. 7a. Figure 7b shows a direct comparison of our theory with experimental results.[24,25] The best agreement was obtained for the parameters $\alpha = 9$ and $\varepsilon = 0.8$.

The correlation of the results of the theory with the theoretical data turned out to be much higher than for other published high-elasticity theories (see Ref. 16). The fact that $\varepsilon < 1$ in both cases is not surprising and is due to the fact that the methods used in Refs. 24 and 25 to prepare the polymer net cannot be regarded as equivalent to instantaneous crosslinking.

3. The following experimental fact is well known in high-elasticity physics: when the $\tau(\lambda)$ dependence is investigated for uniaxial tension or compression of partially swol-
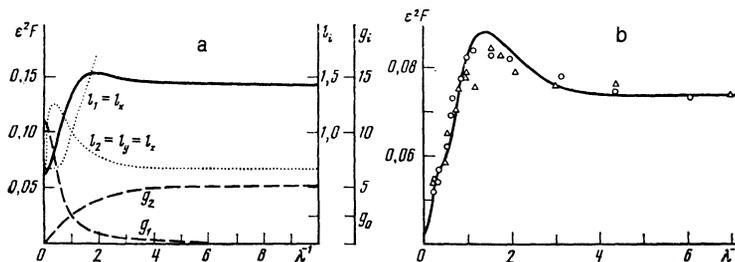

FIG. 7. Uniaxial tension and compression of a dry polymer net: a—calculated plots of $g_{1,2}(\lambda^{-1})$, $l_{1,2}(\lambda^{-1})$ and $\xi/(N/G_0) \equiv \varepsilon^2 F(\lambda^{-1}, \alpha, \varepsilon)$ at $\alpha = 12$ and $\varepsilon = 1$; b—comparison of the results of the theory (solid line) and the experimental results of Refs. 24 (circles) and 25 (triangles). The best agreement (correlation coefficient better than 0.99 in both cases) is reached by choosing the parameters $\alpha = 9$, $\varepsilon = 0.8$ and an ordinate scale corresponding to $\nu NT/V_0 G_0 = 1.35 \cdot 10^{-4}$ Pa for polydimethylsiloxane nets (Ref. 24) and $\nu NT/V_0 G_0 = 2.27 \cdot 10^{-4}$ Pa for natural rubber (Ref. 25).
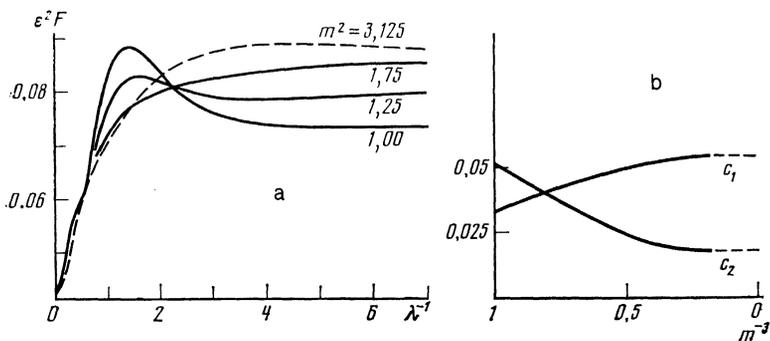
FIG. 8. Uniaxial tension–compression of swollen polymer net: a—plots of $\xi'/(N/G_0)\equiv\varepsilon^2 F(\lambda^{-1}, \alpha\ \varepsilon m^2)$ at $\alpha = 9$ and $\varepsilon = 0.8$ for different values of m; b—dependences of the Mooney-Rivlin parameters c_1 and c_2 on the degree of swelling m^{-3}.

len polymer nets, the deviations from the corresponding classical behavior turn out to be much less pronounced and decrease with increasing degree of swelling (see, e.g., Ref. 9). To be able to describe the principal high-elasticity-physics effects connected with topological restrictions, our theory must automatically account for this fact. Consider uniaxial tension and compression of a net (having the same parameters as in Fig. 7b) subjected to preliminary isotropic swelling by m times: $\lambda_x = m\lambda$, $\lambda_y = \lambda_z = m\lambda^{-1/2}$. In this case classical theory yields for the stress the expression [cf. (1)] $\tau_0' = vTm^2(\lambda - \lambda^{-2})/V$. It is therefore convenient to represent the experimental results in modified Mooney-Rivlin coordinates[3] $\xi' = \tau/\tau_0' - \lambda^{-1}$. A family of calculated plots of $\xi'(\lambda^{-1})$ for different values of m is shown in Fig. 8a. It can be seen that as m is increased the deviations from the classical theory indeed become less pronounced. Figure 8b shows, as functions of the degree of swelling, the phenomenological parameters c_1 and c_2 that can be determined from an analysis of the curves of Fig. 8a (in accord with $\xi' = (N/G_0)$ $(c_1 + \lambda^{-1}c_2)$, the approximation by a straight line was carried out in the interval $0.55 < \lambda^{-1} < 0.95$). At not too large values of m, these plots agree well with the known experimental data (see, e.g., Ref. 9).

To demonstrate how our theory describes the dependence of the net properties on the conditions of its preparation, we consider the results for uniaxial tension and compression of a dry net obtained by instantaneous crosslinking in a concentrated polymer solution, after which the solvent was removed. As noted above, it is necessary to use for the free energy of the net Eq. (37) [in place of (35)]. A family of

the $\tau(\lambda)$ curves in Mooney-Rivlin coordinates is shown for this case at different values of the parameter ε in Fig. 9. It can be seen that, compared with the case of crosslinking in a dry state ($\varepsilon = 1$), the function $\xi(\lambda^{-1})$ acquires a steeper maximum; when ε decreases this maximum shifts towards smaller λ^{-1}. We note also the appearance, at small ε, of an additional singularity on the $\xi(\lambda^{-1})$ curve in the region $0.1 < \lambda^{-1} < 0.4$. When ε decreases the constants c_1 and c_2 decrease, in agreement with experiment.[9]

5. If we consider the general case of uniaxial tension or compression of a partially swollen polymer network ($m \neq 1$), prepared in the presence of a solvent ($\varepsilon \neq 1$), the $\tau(\lambda)$ that results from our theory has the following structure:

$$\tau = (vNT/G_0 V)\, m^2 (\lambda - \lambda^{-2})\, \varepsilon^2 F(\lambda^{-1}, \alpha, \varepsilon m^2).$$

The curves in Figs. 7–9 illustrate the dependences of the function $F(\lambda^{-1}, \alpha, \varepsilon m^2)$ on all its arguments. We note that as $\lambda^{-1} \to 0$ this function approaches a value $F = 4/27g_0$ that is independent of εm^2. If $\varepsilon m^2 > 2.5$, the dependence on this argument becomes very weak at all values of λ^{-1}.

We can conclude thus that the molecular theory developed in this paper accounts for a large number of experimental facts. In particular, it explains the Mooney-Rivlin formula and the decrease of the corrections to the classical theory made necessary by the swelling of the polymer nets, and describes in terms molecular theory the dependence of the net properties on the preparation conditions. The earlier theories of high elasticity of polymer net with account taken of topological restrictions[9–15] could not account for so large a number of experimental facts. Therefore further generalization and refinement of the present analysis, as well as its applications to other types of elastic deformation and of conditions of obtaining polymer net appears to be of great interest.

FIG. 9. Uniaxial tension–compression of dry polymer net prepared in the absence of a solvent. The function $\varepsilon^2 F(\lambda^{-1}, \alpha, \varepsilon) \equiv \xi(N/G_0)^{-1}$ at $\alpha = 9$ and different values of ε.

[1] At $k = \Sigma_i k_i \gg 1$ the width of the maximum is much smaller than the number k of the primitive-path steps; the reason is that, on the one hand, k is proportional to N, and on the other, the distribution over this quantity is governed by the presence of random loops of the coarsened trajectory, i.e., is diffusive.

[2] The parameter ε decreases with decreasing volume fraction Φ_0 of the polymer in the solution under the crosslinking conditions. For example, for crosslinking in a semidilute solution ($\Phi_0 \ll 1$) it can be shown that $\varepsilon \sim \Phi_0^{1/3}$.
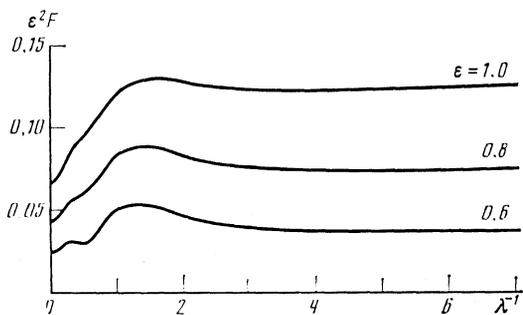
F. F. Ternovskiĭ and A. R. Khokhlov   735

[3] The definition of the stress $\tau = (1/V)(\partial \mathscr{F}/\partial \lambda)_m$ is the same as before, but $V = m^3 V_0$ is the volume of the swollen sample.

[1] P. G. De Gennes, *Scaling Concepts in Polymer Physics*, Cornell Univ. Press, 1979.

[2] H. M. James and E. Guth, J. Chem. Phys. **11**, 455 (1943).

[3] P. J. Flory and J. Rehner, *ibid.*, p. 512.

[4] F. T. Wall, *ibid.*, p. 527.

[5] L. Treloar, Trans. Faraday Soc. 1943, **39**, 36.

[6] L. Treloar, *The Physics of Rubber Elasticity*, 3rd ed., Clarendon Press, Oxford, 1975.

[7] M. J. Mooney, Appl. Phys. **11**, 582 (1940).

[8] R. S. Rivlin, Phil. Trans. Roy. Soc. **241A**, 379 (1948).

[9] L. S. Priss, High-Elasticity Theory. Status and Trends in Its Further Development, NTsBI, Pushchino, 1981.

[10] L. S. Priss, Pure Appl. Chem. **53**, 1581 (1981).

[11] G. Marucci, Macromolecules **14**, 434 (1981).

[12] S. F. Edwards, Brit. Polym. J. **9**, 140 (1977).

[13] R. J. Gaylord, Polym. Bull. **9**, 181 (1983).

[14] W. W. Graessley, Adv. Polym. Sci. **46**, 67 (1982).

[15] R. C. Ball, M. Doi, S. F. Edwards, and M. Warner, Polymer **22**, 1010 (1981).

[16] M. Gottlieb and R. J. Gaylord, Polymer **24**, 1644 (1983).

[17] M. Gottlieb and R. J. Gaylord, Macromolecules **17**, 2024 (1984).

[18] A. Yu. Groserg and A. R. Khokhlov, Unsolved Problems of the Statistical Physics of Macromolecules [in Russian], NTsBI, Pushchino, 1985.

[19] E. Helfand and D. S. Pearson, J. Chem. Phys. **79**, 2054 (1983).

[20] M. Rubenstein and E. Helfand, *ibid.* **82**, 2477 (1985).

[21] A. R. Khokhlov and S. K. Nechaev, Phys. Lett. **A112**, 156 (1985).

[22] M. K. Koleva, A. N. Semenov, and A. R. Khokhlov, in: Mathematical Methods for Polymer Research [in Russian], NTsBI, Pushchino, 1985, p. 12.

[23] R. W. Brotzman and B. E. Eichinger, Macromolecules **15**, 531 (1982).

[24] H. Pak and P. J. Flory, J. Polym. Sci: Polym. Phys. Ed. **17**, 1845 (1979).

[25] R. S. Rivlin and D. W. Saunders, Phil. Trans. Roy. Soc. **243A**, 251 (1951).

Translated by J. G. Adashko

736   Sov. Phys. JETP 63 (4), April 1986

F. F. Ternovskiĭ and A. R. Khokhlov   736